AGARD-R-575-70

AGARD-R-575-70

AGARD

ADVISORY GROUP FOR AEROSPACE RESEARCH & DEVELOPMENT

7 RUE ANCELLE 92 NEUILLY-SUR-SEINE FRANCE

AGARD REPORT No. 575

on

Test Cases for Numerical Methods in Two-Dimensional Transonic Flows

by

R. C. Lock

NORTH ATLANTIC TREATY ORGANIZATION

DISTRIBUTION AND AVAILABILITY
ON BACK COVER

AGARD Report No. 575

NORTH ATLANTIC TREATY ORGANIZATION

ADVISORY GROUP FOR AEROSPACE RESEARCH AND DEVELOPMENT

(ORGANISATION DU TRAITE DE L'ATLANTIQUE NORD)

TEST CASES FOR NUMERICAL METHODS IN TWO-DIMENSIONAL TRANSONIC FLOWS

Compiled by R. C. Lock

Aerodynamics Division, National Physical Laboratory, Teddington

This Report was prepared at the request of the
Fluid Dynamics Panel of AGARD

This document has been reproduced directly
from copy set and supplied by the author.

Published November 1970

533.69.01:533.6.011.35

Printed by Technical Editing and Reproduction Ltd
Harford House, 7-9 Charlotte St, London. W1P 1HD

CONTENTS

LIST OF SYMBOLS

M	Local Mach number
M_∞	Free stream Mach number
α	Angle of incidence (degrees); also parameter in method of Ref. 3.
x	Chordwise co-ordinate
y	Normal co-ordinate
t	Maximum thickness of aerofoil
c	Aerofoil chord
C_p	Pressure coefficient
C_p^*	Critical pressure coefficient ($M = 1$)
C_L	Lift coefficient
θ	Surface slope
s	Distance along surface
τ	Velocity parameter (see Ref. 3)
ε_o, α, T, τ_1, τ_c, θ_c, μ_2	Parameters in method of Ref. 3

SUMMARY

In order to provide test cases for the development of numerical methods for the computation of two-dimensional transonic flows round aerofoils, 6 aerofoil shapes have been selected for which accurate solutions are available. These include both symmetrical and cambered profiles, non-lifting and lifting, in subcritical and supercritical (shock-free) flow.

1. Introduction

At the Specialists' Meeting on transonic aerodynamics,[1] held by AGARD in Paris during September 1968, a number of papers were presented describing developments currently in progress on numerical methods for calculating inviscid transonic flows round aerofoil sections in two dimensions. Even though most of these methods use the full equations of motion without simplification, there are a number of factors - the discretisation of the partial differential equations, the numerical techniques used to solve them, and the approximations to the boundary conditions on the aerofoil and at infinity - which will all tend to introduce errors of unknown magnitude which it is difficult to estimate purely from internal considerations.

At discussions held during the meeting, and confirmed by the subsequent Technical Evaluation Report [2], it was suggested that a set of test cases should be issued by AGARD in order to provide checks of the accuracy of the various methods proposed.

In considering the choice of these test cases, it is clearly essential that accurate theoretical results should be available for the chosen shapes; experimental results are usually unsatisfactory because of the presence of viscous effects and of wind tunnel constraints. It is also desirable that examples should be included of both lifting and non-lifting aerofoils, with and without camber, and in subcritical and supercritical flow. For this purpose it is considered that only two existing methods can provide the requisite accuracy. These are:-

(a) The hodograph method of Nieuwland[3] (NLR)

In this method solutions are calculated for both the aerofoil shapes and pressure distribution, neither of which can be specified in advance; but by varying a number of basic parameters a large variety of shapes can be obtained which are of practical interest, and both subcritical and supercritical (shock-free) flows can be considered. The method in its latest form is capable of designing lifting (cambered) aerofoils, and although most of the examples suggested below are symmetrical profiles at zero incidence, one lifting supercritical case has also been included.

(b) The finite-difference method of Sells[4] (RAE)

In this method solutions for subcritical flow about any given aerofoil shape are obtained by a finite difference procedure, first mapping the region external to the aerofoil conformally into the interior of a unit circle. Great care has been taken in satisfying the boundary conditions and in minimising the finite difference and truncation errors involved in the numerical solution; and it is believed both from internal checks and comparisons with examples calculated by Nieuwland's method (for subcritical flow) that an accuracy of the order of 1% of the maximum perturbation velocity is usually obtained. The method is limited to a maximum local Mach number of about 0·98; but lifting, cambered aerofoils can be treated without difficulty.

The two methods described above have thus provided us with definite solutions for arbitrary aerofoils in subcritical flow, and for particular aerofoils in shock-free supercritical flow. In general, of course, supercritical flows will involve shock waves of appreciable strength, and indeed most of the methods described in the conference proceedings [1] are intended eventually to deal with such cases. It is, however, clearly impossible to provide any definitive solution for reference purposes. The only sensible course to adopt would therefore seem to be to suggest a few cases for a standard aerofoil (e.g. NACA 0012) for which numerical results obtained by different workers could be compared, and for which reliable wind tunnel results might be available; to minimise the effects of viscosity and tunnel constraint in the latter, the choice of zero incidence is indicated. No actual wind tunnel results are included here, but experiments on NACA 0012 for tunnel calibration purposes are currently in progress at NPL and ONERA.

2. Test Cases

2.1 Specification : Aerofoils and pressure distributions

	No.	Designation	Thickness/ Chord	Free stream Mach No.	Incidence	Max. local Mach No.	Location: Ordinates	Location: Pressure distribution	
							Table	Table	Fig.
(i) Subcritical									
(a) Symmetric	1(a)	NACA 0012	0·12	0·72	0	0·985	(Ref.5)	1	1
	2	NLR 0·10-0·75-1·25	0·1253	0·7454	0	0·982	2	2	2
(b) Lifting	1(b)	NACA 0012	0·12	0·63	2°	0·983	(Ref.5)	1	3
(ii) Supercritical									
(a) Symmetric	3	NLR 0·11-0·75-0·9	0·1137	0·786	0	1·060	3	3	4
	4	0·11-0·75-1·25	0·1162	0·786	0	1·136	4	4	5
	5	0·1025-0·675-1·375	0·1578	0·756	0	1·291	5	5	6
(b) Lifting	6	NLR $\begin{cases} \varepsilon_o = \cdot 625, \alpha = \cdot 0275, T = \cdot 375 \\ \tau_1 = \cdot 1025, \tau_c = \cdot 06226 \\ \theta_c = -1\cdot 1855°, \mu_2 = \cdot 4 \end{cases}$	0·1212	0·756	1·32°	1·202	6	6	7

The suggested examples are detailed in the list above; these comprise:-

3 subcritical cases (2 aerofoils), of which one is calculated by the method of Ref. 3 and chosen from the collection of Ref. 6, and 2 are calculated, for one representative aerofoil shape, by the method of Ref. 4;

and 4 supercritical cases, of which 3 symmetrical aerofoils have been chosen from the collection of Ref. 7, and one (a cambered lifting aerofoil) has been kindly supplied by NLR (unpublished). These 3 symmetrical examples have been selected with progressively increasing values of the maximum local Mach number, and thus provide an increasingly severe test of any numerical method for the direct problem.

These supercritical examples are of course free from shock waves. To cover the case when appreciable shock waves would be present (for which, as mentioned in the Introduction, no definitive solution can yet be provided) it is suggested that the NACA 0012 section should be used, at zero incidence; the critical Mach number for this section is between ·72 and ·73, so that calculations from (say) M_∞ = ·72 to 0·80 should show the gradual development of the shock wave up to an appreciable strength. Even at the higher Mach number (·80), however, separation of the turbulent boundary layer is not caused by the shock at Reynolds numbers above 2×10^6, so that experimentally measured pressure distributions should not be subject to serious viscous effects, and would therefore provide a valid comparison with theory. No experimental measurements are quoted here (they are still being refined); it is suggested that calculations should be made with M_∞ = ·725, ·75, ·775 and ·80 so that the results of different methods can be compared with each other and, later, with experiment.

2.2 Interpolation of aerofoil ordinates

In any direct method for calculating the flow field produced by a given aerofoil, particularly when a comparison between the results of different techniques is intended as is the present case, it is clearly necessary that a reliable and unique interpolation procedure should be used to define the aerofoil ordinates at arbitrary points not included in the tables. It is suggested that the following methods might be used:-

(a) NACA 0012

This is specified analytically in Ref. 5, so the question of interpolation does not arise. Note, however, that, because the formula of Ref. 5 gives a non-zero value of the thickness at $x = 1$, the aerofoil has been extended to give a trailing edge of zero thickness at $x = 1{\cdot}0089$; this explains why the pressure distribution output given in Table 1 extends up to this value of x.

(b) NLR aerofoils

It is recommended in the Appendix to Ref. 7 that a fifth degree interpolation formula should be used, making use of the tabulated slopes and curvatures provided for these aerofoils; this formula is reproduced below.

Suppose that x lies between two tabulated values x_{i-1}, x_i,

and write

$$y_i = y(x_i) \quad \text{and so on},$$

$$y_i' = \tan\theta_i \quad \text{(local slope)},$$

$$y_i'' = -\left(1 + y_i'^2\right)^{3/2}\left(\frac{d\theta}{ds}\right)_i .$$

Writing also

$$\xi = x - x_{i-1}$$

$$h_i = x_i - x_{i-1},$$

the interpolation formula is

$$y(x) = a_0 + a_1\xi + a_2\xi^2 + \xi^3\left[a_3 + a_4(\xi - h_i) + a_5(\xi - h_i)^2\right]$$

where

$$a_0 = y_{i-1}$$

$$a_1 = y_i{}'_{-1}$$

$$a_2 = \tfrac{1}{2}\, y''_{i-1}$$

$$a_3 = \frac{1}{h_i^3}\left[y_i - y_{i-1} - h_i\, y'_{i-1} - \tfrac{1}{2} h_i^2\, y''_{i-1} \right]$$

$$a_4 = \frac{1}{h_i^4}\left[-3y_i + 3y_{i-1} + h_i\,(y_i' + 2y'_{i-1}) + \tfrac{1}{2} h_i^2\, y''_{i-1} \right]$$

$$a_5 = \frac{1}{h_i^5}\left[6y_i - 6y_{i-1} - 3h_i\,(y_i' + y'_{i-1}) + \tfrac{1}{2} h_i^2\,(y_i'' - y'_{i-1}) \right]$$

3. Concluding remarks

The examples suggested above should provide a set of test cases, as comprehensive as is possible at the present time, which may be regarded as providing definitive solutions to the problem of calculating the inviscid transonic flow round a two-dimensional aerofoil in a subsonic free stream. It is hoped that those who are engaged in the development of finite-difference methods for this problem will consider including some or all of these test cases in their programme; if the results of such comparisons could then be communicated to AGARD (via the Secretary, Fluid Motion Panel), a comparative review could then be issued which should be of mutual benefit to all concerned.

References

No.	Author(s)	Title, etc.
1	-	Transonic Aerodynamics. AGARD Conference Proceedings No. 35. September 1968.
2	D. Küchemann	Technical Evaluation Report on AGARD Specialists' Meeting on Transonic Aerodynamics. 1969.
3	G. Y. Nieuwland	Transonic potential flow round a family of quasi-elliptic aerofoil sections. NLR-TR T.172. 1967.
4	C. C. L. Sells	Plane subcritical flow past a lifting aerofoil. R.A.E. Tech. Rep. 67146. 1967.
5	I. H. Abbott and A. E. Von Doehnhoff	Theory of wing sections (p.113) McGraw-Hill. 1949.
6	J. W. Boerstoel	Symmetric subsonic potential flows around quasi-elliptical aerofoil sections. NLR TR 68016 U.
7	H. W. Baurdoux and J. W. Boerstoel	Symmetrical transonic potential flow around quasi-elliptical aerofoil sections. NLR TR 69007 U.

Table 1

Aerofoil NACA 0012

1(a)

$\alpha = 0$ $M_\infty = 0{\cdot}7200$

x/c	Mach No.	C_p
1·009	0·0000	1·13640
1·005	0·5499	0·41339
0·995	0·5985	0·29922
0·978	0·6305	0·22220
0·956	0·6561	0·15942
0·929	0·6784	0·10426
0·897	0·6982	0·05481
0·860	0·7166	0·00861
0·820	0·7340	−0·03521
0·776	0·7508	−0·07784
0·729	0·7675	−0·12001
0·680	0·7843	−0·16270
0·630	0·8018	−0·20699
0·578	0·8199	−0·25295
0·525	0·8392	−0·30170
0·473	0·8595	−0·35294
0·421	0·8809	−0·40664
0·371	0·9032	−0·46245
0·322	0·9257	−0·51824
0·275	0·9475	−0·57212
0·230	0·9672	−0·62026
0·189	0·9807	−0·65316
0·151	0·9837	−0·66042
0·117	0·9748	−0·63874
0·086	0·9517	−0·58233
0·060	0·9172	−0·49735
0·039	0·8647	−0·36596
0·022	0·7860	−0·16702
0·010	0·6397	0·19960
0·002	0·3761	0·77432

$C_p^* = -0{\cdot}6996$

1(b)

$\alpha = 2{\cdot}0000°$ $M_\infty = 0{\cdot}6300$

x/c	Mach No.	C_p
Lower surface		
1·009	0·0000	1·10320
1·005	0·4912	0·38817
0·995	0·5308	0·28208
0·978	0·5560	0·21247
0·956	0·5754	0·15783
0·929	0·5916	0·11161
0·897	0·6054	0·07175
0·860	0·6178	0·03587
0·820	0·6289	0·00315
0·776	0·6393	−0·02742
0·729	0·6491	−0·05641
0·680	0·6585	−0·08449
0·630	0·6678	−0·11230
0·578	0·6769	−0·13962
0·525	0·6860	−0·16685
0·473	0·6947	−0·19326
0·421	0·7030	−0·21820
0·371	0·7104	−0·24066
0·322	0·7163	−0·25866
0·275	0·7202	−0·27057
0·230	0·7215	−0·27423
0·189	0·7188	−0·26630
0·151	0·7114	−0·24376
0·117	0·6981	−0·20338
0·086	0·6762	−0·13738
0·060	0·6431	−0·03865
0·039	0·5918	0·11122
0·022	0·5113	0·33499
0·010	0·3716	0·67553
0·002	0·1284	1·04931
Upper surface		
0·000	0·2277	0·93650
0·002	0·6002	0·08690
0·010	0·8489	−0·66381
0·022	0·9499	−0·96815
0·039	0·9747	−1·04142
0·060	0·9828	−1·06501
0·086	0·9739	−1·03888
0·117	0·9570	−0·98915
0·151	0·9337	−0·92004
0·189	0·9093	−0·84702
0·230	0·8844	−0·77192
0·275	0·8597	−0·69693
0·322	0·8360	−0·62452
0·371	0·8133	−0·55510
0·421	0·7917	−0·48879
0·473	0·7713	−0·42649
0·525	0·7522	−0·36802
0·578	0·7342	−0·31310
0·630	0·7173	−0·26172
0·680	0·7012	−0·21274
0·729	0·6857	−0·16591
0·776	0·6705	−0·12016
0·820	0·6552	−0·07446
0·860	0·6395	−0·02804
0·897	0·6231	0·02031
0·929	0·6055	0·07152
0·956	0·5860	0·12784
0·978	0·5634	0·19178
0·995	0·5354	0·26961
1·005	0·4932	0·38277

$C_p^* = -1{\cdot}1151$ $C_L = 0{\cdot}335$

Table 2

NLR Quasi-Elliptical Aerofoil Section 0·1000 - 0·7500 - 1·2500
Profile Number 3
Free Stream Mach Number 0·7454

τ	x	y	C_p	Mach No.	θ	Curvature = $\frac{d\theta}{ds}$
0·0000	-1·77989	0·00000	1·1467	0·0000	1·57080	10·078
0·0100	-1·77704	0·02360	1·0182	0·2247	1·330	10·13
0·0200	-1·77419	0·03310	0·8929	0·3194	1·230	10·19
0·0300	-1·77135	0·04020	0·7707	0·3932	1·1514	10·26
0·0400	-1·76852	0·04604	0·6517	0·4564	1·0846	10·33
0·0500	-1·76567	0·05106	0·5357	0·5130	1·0247	10·41
0·0600	-1·76280	0·05549	0·4227	0·5649	0·9696	10·48
0·0700	-1·75990	0·05950	0·3127	0·6135	0·9176	10·53
0·0800	-1·75693	0·06319	0·2056	0·6594	0·8676	10·54
0·0900	-1·75384	0·06665	0·1014	0·7032	0·8188	10·48
0·1000	-1·75057	0·06998	0·0000	0·7454	0·7701	10·30
0·1100	-1·74696	0·07331	-0·0986	0·7861	0·721	9·91
0·1200	-1·74277	0·07680	-0·1945	0·8257	0·668	9·25
0·1300	-1·73742	0·08077	-0·2877	0·8644	0·611	8·15
0·1400	-1·72932	0·08601	-0·3783	0·9022	0·540	6·45
0·1488	-1·71432	0·09403	-0·4560	0·9350	0·448	4·25
0·1500	-1·71071	0·09574	-0·4662	0·9393	0·435	3·862
0·1521	-1·70185	0·09967	-0·4842	0·9470	0·401	3·15
0·1544	-1·68438	0·10655	-0·5045	0·9556	0·351	2·25
0·1563	-1·65900	0·11506	-0·5199	0·9623	0·300	1·55
0·1579	-1·62050	0·12584	-0·5337	0·9682	0·249	1·017
0·1595	-1·55963	0·13957	-0·5471	0·9739	0·198	0·638
0·1600	-1·53016	0·14522	-0·5517	0·9759	0·181	0·5359
0·1601	-1·52553	0·14606	-0·5523	0·9762	0·180	0·522
0·1607	-1·48363	0·15326	-0·5572	0·9783	0·160	0·425
0·1612	-1·43179	0·16109	-0·5615	0·9801	0·140	0·3440
0·1615	-1·36741	0·16949	-0·5646	0·9815	0·120	0·2772
0·1617	-1·28730	0·17831	-0·5658	0·9820	0·0	0·2231
0·1615	-1·18764	0·18727	-0·5642	0·9813	0·0800	0·1802
0·1608	-1·06473	0·19583	-0·5588	0·9790	0·0599	0·1471
0·1600	-0·95740	0·20146	-0·5517	0·9759	0·0452	0·128213
0·1596	-0·91551	0·20324	-0·5484	0·9745	0·0400	0·12250
0·1577	-0·73903	0·20850	-0·5323	0·9676	0·02001	0·10526
0·1551	-0·53879	0·21047	-0·5100	0·9580	0·00007	0·09439
0·1517	-0·31818	0·20825	-0·4807	0·9455	-0·02003	0·08893
0·1500	-0·22167	0·20590	-0·4662	0·9393	-0·02853	0·087936
0·1475	-0·09097	0·20143	-0·4448	0·9302	-0·03996	0·08776
0·1400	0·23993	0·18330	-0·3783	0·9022	-0·06978	0·092717
0·1300	0·56745	0·15519	-0·2877	0·8644	-0·10207	0·104502
0·1200	0·81083	0·12697	-0·1945	0·8257	-0·1293	0·1170
0·1100	0·99803	0·10048	-0·0986	0·7861	-0·152	0·122
0·1000	1·14592	0·07639	0·0000	0·7454	-0·171	0·124
0·0900	1·26468	0·05499	0·1014	0·7032	-0·185	0·110
0·0800	1·36175	0·03634	0·2056	0·6594	-0·1934	0·0376
0·0700	1·44155	0·02074	0·3127	0·6135	-0·1903	-0·13351
0·0600	1·50762	0·00857	0·4227	0·5649	-0·1686	-0·6042
0·0500	1·56244	0·00081	0·5357	0·5130	-0·091	-2·893
0·0472	1·57650	0·00000	0·5679	0·4977	0·00000	

Table 3

NLR Quasi-Elliptical Aerofoil Section 0·1100 - 0·7500 - 0·9000
Profile Number 8
Free Stream Mach Number 0·7861

τ	x	y	C_p	Mach No.	θ	Curvature = $\frac{d\theta}{ds}$
0·00000	-1·79504	0·00000	1·1642	0·0000	1·57080	49·100807
0·01000	-1·79307	0·00918	1·0440	0·2247	1·18	30·8
0·02000	-1·79046	0·01432	0·9269	0·3194	1·031	21·5
0·03000	-1·78714	0·01920	0·8127	0·3932	0·923	15·79
0·04000	-1·78303	0·02414	0·7014	0·4564	0·834	12·01
0·05000	-1·77798	0·02928	0·5930	0·5130	0·758	9·33
0·06000	-1·77184	0·03470	0·4874	0·5649	0·6904	7·34
0·07000	-1·76437	0·04048	0·3845	0·6135	0·6287	5·822
0·08000	-1·75528	0·04668	0·2844	0·6594	0·5716	4·630
0·09000	-1·74418	0·05340	0·1870	0·7032	0·5181	3·681
0·10000	-1·73052	0·06073	0·0922	0·7454	0·4674	2·916
0·11000	-1·71360	0·06873	0·0000	0·7861	0·4190	2·295
0·12000	-1·69241	0·07756	-0·0896	0·8257	0·3724	1·7910
0·13000	-1·66555	0·08733	-0·1768	0·8644	0·32736	1·3831
0·14000	-1·63114	0·09815	-0·2614	0·9022	0·28406	1·05582
0·15000	-1·58661	0·11009	-0·3437	0·9393	0·24180	0·79811
0·16000	-1·52848	0·12310	-0·4235	0·9759	0·20059	0·59896
0·16667	-1·47946	0·13236	-0·4754	1·0000	0·17360	0·49208
0·17000	-1·45077	0·13718	-0·5010	1·0120	0·16001	0·44399
0·17500	-1·39976	0·14485	-0·5389	1·0299	0·13901	0·37417
0·18000	-1·32987	0·15376	-0·5762	1·0476	0·11539	0·297747
0·18167	-1·29638	0·15748	-0·5886	1·0536	0·10591	0·267000
0·18333	-1·24843	0·16228	-0·6008	1·0595	0·09399	0·229433
0·18333	-0·94118	0·18268	-0·6008	1·0595	0·04422	0·120369
0·18167	-0·83289	0·18680	-0·5886	1·0536	0·03194	0·106563
0·18000	-0·73948	0·18933	-0·5762	1·0476	0·02239	0·098506
0·17833	-0·65319	0·19090	-0·5639	1·0417	0·01414	0·093190
0·17667	-0·57171	0·19175	-0·5514	1·0358	0·00670	0·089533
0·17500	-0·49395	0·19200	-0·5389	1·0299	-0·00016	0·086994
0·17333	-0·41934	0·19175	-0·5263	1·0239	-0·00658	0·085257
0·17167	-0·34754	0·19106	-0·5137	1·0179	-0·01266	0·084117
0·17000	-0·27837	0·18998	-0·5010	1·0120	-0·01845	0·083436
0·16667	-0·14708	0·18684	-0·4754	1·0000	-0·02938	0·083092
0·16417	-0·05444	0·18376	-0·4561	0·9910	-0·03709	0·083498
0·16167	0·03372	0·18016	-0·4366	0·9819	-0·04449	0·084339
0·16000	0·09011	0·17752	-0·4235	0·9759	-0·04928	0·085101
0·15833	0·14468	0·17470	-0·4104	0·9698	-0·05395	0·086004
0·15667	0·19748	0·17173	-0·3972	0·9638	-0·05853	0·087030
0·15500	0·24861	0·16861	-0·3839	0·9577	-0·06301	0·088171
0·15333	0·29799	0·16539	-0·3705	0·9516	-0·06741	0·089412
0·15167	0·34589	0·16205	-0·3571	0·9455	-0·07173	0·090744
0·15000	0·39217	0·15863	-0·3437	0·9393	-0·07597	0·092156
0·14750	0·45876	0·15335	-0·3233	0·9301	-0·08220	0·094401
0·14500	0·52204	0·14795	-0·3028	0·9208	-0·08827	0·096768
0·14250	0·58223	0·14244	-0·2822	0·9115	-0·09419	0·099225
0·14000	0·63943	0·13687	-0·2614	0·9022	-0·09997	0·101737
0·13750	0·69383	0·13126	-0·2405	0·8928	-0·1056	0·1043
0·13500	0·74555	0·12563	-0·2194	0·8834	-0·1111	0·1068
0·13250	0·79471	0·12002	-0·1982	0·8739	-0·1164	0·1092
0·13000	0·84152	0·11442	-0·1768	0·8644	-0·122	0·112
0·12667	0·90033	0·10703	-0·1480	0·8516	-0·128	0·116
0·12333	0·95545	0·09974	-0·1190	0·8387	-0·135	0·115
0·12000	1·00698	0·09258	-0·0896	0·8257	-0·141	0·117
0·11500	1·07833	0·08214	-0·0451	0·8061	-0·150	0·120
0·11000	1·14317	0·07210	0·0000	0·7861	-0·158	0·118
0·10500	1·20234	0·06249	0·0458	0·7659	-0·165	0·113
0·10000	1·25596	0·05332	0·0922	0·7454	-0·172	0·111
0·09000	1·35001	0·03656	0·1870	0·7032	-0·1786	0·0520
0·08000	1·42858	0·02234	0·2844	0·6594	-0·17808	-0·070293
0·07000	1·49459	0·01079	0·3845	0·6135	-0·16506	-0·37512
0·06500	1·52352	0·00617	0·4356	0·5896	-0·14975	-0·7015
0·06000	1·55001	0·00250	0·4874	0·5649	-0·1229	-1·3626
0·05285	1·58224	0·00000	0·5626	0·5282	0·00000	

Table 4

NLR Quasi-Elliptical Aerofoil Section 0·1100 – 0·7500 – 1·2500
Profile Number 6
Free Stream Mach Number 0·7861

τ	x	y	C_p	Mach No.	θ	Curvature = $\frac{d\theta}{ds}$
0·00000	−1·79504	0·00000	1·1642	0·0000	1·57080	9·317575
0·01000	−1·79217	0·02463	1·0440	0·2247	1·339	9·35
0·02000	−1·78932	0·03453	0·9269	0·3194	1·242	9·40
0·03000	−1·78650	0·04192	0·8127	0·3932	1·168	9·46
0·04000	−1·78369	0·04797	0·7014	0·4564	1·105	9·53
0·05000	−1·78090	0·05314	0·5930	0·5130	1·048	9·60
0·06000	−1·77813	0·05767	0·4874	0·5649	0·997	9·69
0·07000	−1·77538	0·06172	0·3845	0·6135	0·9494	9·79
0·08000	−1·77263	0·06539	0·2844	0·6594	0·9044	9·88
0·09000	−1·76987	0·06874	0·1870	0·7032	0·8613	9·96
0·10000	−1·76709	0·07184	0·0922	0·7454	0·8197	10·01
0·11000	−1·76426	0·07475	0·0000	0·7861	0·7790	10·01
0·12000	−1·76133	0·07754	−0·0896	0·8257	0·7387	9·928
0·13000	−1·75823	0·08025	−0·1768	0·8644	0·6981	9·717
0·14000	−1·75483	0·08298	−0·2614	0·9022	0·6565	9·310
0·15000	−1·75091	0·08586	−0·3437	0·9393	0·6127	8·647
0·16000	−1·74603	0·08912	−0·4235	0·9759	0·5647	7·655
0·16667	−1·74181	0·09169	−0·4754	1·0000	0·5297	6·772
0·17000	−1·73918	0·09319	−0·5010	1·0120	0·5109	6·259
0·18000	−1·72718	0·09933	−0·5762	1·0476	0·4385	4·491
0·19000	−1·69756	0·11116	−0·6492	1·0830	0·3328	2·4312
0·19333	−1·67876	0·11721	−0·6730	1·0947	0·2916	1·8405
0·19667	−1·65489	0·12383	−0·6966	1·1064	0·2516	1·3921
0·20000	−1·62597	0·13068	−0·7199	1·1180	0·2154	1·05898
0·20167	−1·60850	0·13434	−0·7315	1·1239	0·1978	0·91374
0·20333	−1·58624	0·13858	−0·7430	1·1297	0·1789	0·76322
0·20500	−1·53958	0·14625	−0·7545	1·1355	0·1489	0·53715
0·20500	−1·50975	0·15050	−0·7545	1·1355	0·1344	0·43619
0·20333	−1·44272	0·15869	−0·7430	1·1297	0·10979	0·304970
0·20167	−1·39820	0·16331	−0·7315	1·1239	0·09732	0·255216
0·20000	−1·35734	0·16710	−0·7199	1·1180	0·08754	0·223082
0·19750	−1·29775	0·17195	−0·7024	1·1093	0·07526	0·189977
0·19500	−1·23794	0·17613	−0·6848	1·1005	0·06459	0·166710
0·19250	−1·17688	0·17978	−0·6671	1·0918	0·05496	0·149229
0·19000	−1·11402	0·18295	−0·6492	1·0830	0·04603	0·135506
0·18750	−1·04951	0·18566	−0·6312	1·0742	0·03763	0·124383
0·18500	−0·98246	0·18792	−0·6130	1·0653	0·02962	0·115105
0·18250	−0·91303	0·18971	−0·5947	1·0565	0·02191	0·107210
0·18000	−0·84082	0·19102	−0·5762	1·0476	0·01442	0·100421
0·17833	−0·79105	0·19161	−0·5639	1·0417	0·00952	0·096435
0·17667	−0·73988	0·19197	−0·5514	1·0358	0·00468	0·092856
0·17500	−0·68732	0·19209	−0·5389	1·0299	−0·00012	0·089674
0·17333	−0·63341	0·19196	−0·5263	1·0239	−0·00487	0·086883
0·17167	−0·57824	0·19156	−0·5137	1·0179	−0·00960	0·084479
0·17000	−0·52200	0·19089	−0·5010	1·0120	−0·01429	0·082450
0·16667	−0·40708	0·18871	−0·4754	1·0000	−0·02358	0·079461
0·16417	−0·31976	0·18635	−0·4561	0·9910	−0·03046	0·078069
0·16167	−0·23250	0·18339	−0·4366	0·9819	−0·03724	0·077310
0·16000	−0·17477	0·18111	−0·4235	0·9759	−0·04170	0·077112
0·15833	−0·11767	0·17861	−0·4104	0·9698	−0·04610	0·077129
0·15667	−0·06138	0·17589	−0·3972	0·9638	−0·05046	0·077338
0·15500	−0·00605	0·17297	−0·3839	0·9577	−0·05475	0·077711
0·15333	0·04823	0·16988	−0·3705	0·9516	−0·05899	0·078233
0·15167	0·10127	0·16664	−0·3571	0·9455	−0·06316	0·078882
0·15000	0·15304	0·16326	−0·3437	0·9393	−0·06727	0·079639
0·14750	0·22818	0·15797	−0·3233	0·9301	−0·07332	0·080943
0·14500	0·30026	0·15246	−0·3028	0·9208	−0·07922	0·082405
0·14250	0·36924	0·14679	−0·2822	0·9115	−0·08498	0·083970
0·14000	0·43512	0·14099	−0·2614	0·9022	−0·09058	0·085598
0·13750	0·49800	0·13511	−0·2405	0·8928	−0·0960	0·0873
0·13500	0·55793	0·12917	−0·2194	0·8834	−0·1013	0·0889
0·13250	0·61502	0·12322	−0·1982	0·8739	−0·1065	0·0904
0·13000	0·66941	0·11727	−0·1768	0·8644	−0·111	0·091
0·12667	0·73787	0·10938	−0·1480	0·8516	−0·118	0·093
0·12333	0·80231	0·10155	−0·1190	0·8387	−0·124	0·095
0·12000	0·86255	0·09387	−0·0896	0·8257	−0·130	0·095
0·11667	0·91903	0·08635	−0·0600	0·8126	−0·135	0·095

Table 4 (continued)

τ	x	y	C_p	Mach No.	θ	Curvature = $\frac{d\theta}{ds}$
0·11333	0·97203	0·07901	-0·0302	0·7994	-0·140	0·093
0·11000	1·02106	0·07197	0·0000	0·7861	-0·145	0·091
0·10500	1·09187	0·06139	0·0458	0·7659	-0·151	0·084
0·10000	1·15349	0·05181	0·0922	0·7454	-0·157	0·071
0·09000	1·26405	0·03402	0·1870	0·7032	-0·1612	0·0123
0·08000	1·35614	0·01916	0·2844	0·6594	-0·15672	-0·12424
0·07000	1·43353	0·00757	0·3845	0·6135	-0·13575	-0·48710
0·06500	1·46744	0·00330	0·4356	0·5896	-0·11225	-0·9446
0·06000	1·49854	0·00043	0·4874	0·5649	-0·0637	-2·4983
0·05791	1·51042	0·00000	0·5092	0·5544	0·00000	

Table 5

NLR Quasi-Elliptical Aerofoil Section 0·1025 – 0·6750 – 1·3750
Profile Number 13
Free Stream Mach Number 0·7557

τ	x	y	C_p	Mach No.	θ	Curvature = $\frac{d\theta}{ds}$
0·00000	−1·69058	0·00000	1·1510	0·0000	1·57080	5·962550
0·01000	−1·68599	0·03897	1·0248	0·2247	1·336	5·95
0·02000	−1·68141	0·05473	0·9017	0·3194	1·239	5·94
0·03000	−1·67683	0·06656	0·7817	0·3932	1·163	5·94
0·04000	−1·67225	0·07630	0·6647	0·4564	1·0995	5·94
0·05000	−1·66767	0·08469	0·5508	0·5130	1·0428	5·941
0·06000	−1·66310	0·09208	0·4398	0·5649	0·9911	5·943
0·07000	−1·65851	0·09873	0·3317	0·6135	0·9431	5·944
0·08000	−1·65391	0·10477	0·2265	0·6594	0·8979	5·940
0·09000	−1·64928	0·11033	0·1241	0·7032	0·8550	5·929
0·10000	−1·64460	0·11550	0·0245	0·7454	0·8137	5·904
0·11000	−1·63984	0·12034	−0·0724	0·7861	0·7737	5·858
0·12000	−1·63497	0·12492	−0·1666	0·8257	0·7347	5·787
0·13000	−1·62993	0·12929	−0·2582	0·8644	0·6965	5·671
0·14000	−1·62464	0·13355	−0·3471	0·9022	0·6585	5·509
0·15000	−1·61905	0·13771	−0·4336	0·9393	0·6206	5·282
0·16000	−1·61286	0·14195	−0·5175	0·9759	0·5823	4·991
0·16667	−1·60840	0·14481	−0·5721	1·0000	0·5565	4·760
0·17000	−1·60605	0·14625	−0·5989	1·0120	0·5436	4·633
0·18000	−1·59830	0·15072	−0·6780	1·0476	0·5039	4·225
0·19000	−1·58935	0·15542	−0·7546	1·0830	0·4635	3·797
0·20000	−1·57912	0·16027	−0·8290	1·1180	0·4226	3·402
0·21000	−1·56790	0·16505	−0·9010	1·1529	0·3832	3·1064
0·22000	−1·55664	0·16935	−0·9708	1·1875	0·3468	2·992
0·23000	−1·54660	0·17279	−1·0384	1·2221	0·3145	3·111
0·24000	−1·53798	0·17546	−1·1039	1·2566	0·2863	3·130
0·25000	−1·52414	0·17926	−1·1672	1·2910	0·2521	1·6930
0·25000	−1·48295	0·18874	−1·1672	1·2910	0·2070	0·75233
0·24000	−1·40363	0·20334	−1·1039	1·2566	0·16107	0·44926
0·23000	−1·31607	0·21597	−1·0384	1·2221	0·12744	0·32544
0·22500	−1·26589	0·22200	−1·0049	1·2048	0·11211	0·284110
0·22000	−1·21107	0·22773	−0·9708	1·1875	0·09740	0·251461
0·21500	−1·15159	0·23310	−0·9362	1·1702	0·08318	0·225478
0·21000	−1·08781	0·23797	−0·9010	1·1529	0·06946	0·204587
0·20500	−1·02005	0·24223	−0·8653	1·1355	0·05618	0·187383
0·20000	−0·94843	0·24579	−0·8290	1·1180	0·04329	0·172493
0·19667	−0·89843	0·24774	−0·8044	1·1064	0·03489	0·163222
0·19333	−0·84606	0·24935	−0·7797	1·0947	0·02658	0·154169
0·19000	−0·79100	0·25059	−0·7546	1·0830	0·01835	0·145239
0·18667	−0·73255	0·25141	−0·7293	1·0712	0·01011	0·136536
0·18333	−0·66998	0·25179	−0·7038	1·0595	0·00183	0·128305
0·18000	−0·60268	0·25162	−0·6780	1·0476	−0·00654	0·120864
0·17750	−0·54889	0·25110	−0·6584	1·0388	−0·01291	0·115972
0·17500	−0·49222	0·25018	−0·6388	1·0299	−0·01936	0·111760
0·17250	−0·43282	0·24884	−0·6189	1·0209	−0·02589	0·108267
0·17000	−0·37098	0·24703	−0·5989	1·0120	−0·03250	0·105494
0·16667	−0·28542	0·24387	−0·5721	1·0000	−0·04140	0·102864
0·16333	−0·19766	0·23984	−0·5449	0·9880	−0·05037	0·101343
0·16000	−0·10880	0·23496	−0·5175	0·9759	−0·05936	0·100786
0·15750	−0·04222	0·23077	−0·4967	0·9668	−0·06609	0·100911
0·15500	0·02383	0·22618	−0·4758	0·9577	−0·07278	0·101436
0·15250	0·08893	0·22122	−0·4548	0·9485	−0·07943	0·102308
0·15000	0·15259	0·21594	−0·4336	0·9393	−0·08602	0·103478
0·14750	0·21513	0·21034	−0·4122	0·9301	−0·09254	0·104903
0·14500	0·27584	0·20451	−0·3907	0·9208	−0·09899	0·106546
0·14250	0·33476	0·19847	−0·3690	0·9115	−0·10535	0·108370
0·14000	0·39183	0·19225	−0·3471	0·9022	−0·11163	0·110343
0·13750	0·44699	0·18590	−0·3251	0·8928	−0·11781	0·112434
0·13500	0·50021	0·17944	−0·3030	0·8834	−0·12390	0·114613
0·13250	0·55152	0·17289	−0·2807	0·8739	−0·12989	0·116848
0·13000	0·60092	0·16629	−0·2582	0·8644	−0·1358	0·1192
0·12667	0·66387	0·15744	−0·2279	0·8516	−0·1435	0·1226
0·12333	0·72358	0·14859	−0·1974	0·8387	−0·1509	0·1245
0·12000	0·78037	0·13974	−0·1666	0·8257	−0·158	0·130
0·11667	0·83405	0·13097	−0·1355	0·8126	−0·165	0·129
0·11333	0·88490	0·12230	−0·1041	0·7994	−0·172	0·132
0·11000	0·93307	0·11377	−0·0724	0·7861	−0·179	0·133

Table 5 (continued)

τ	x	y	C_p	Mach No.	θ	Curvature = $\frac{d\theta}{ds}$
0·10500	1·00051	0·10125	−0·0243	0·7659	−0·188	0·134
0·10000	1·06262	0·08914	0·0245	0·7454	−0·197	0·131
0·09500	1·11930	0·07762	0·0739	0·7245	−0·204	0·125
0·09000	1·17250	0·06644	0·1241	0·7032	−0·2100	0·1121
0·08500	1·22095	0·05598	0·1749	0·6815	−0·2150	0·0910
0·08000	1·26560	0·04614	0·2265	0·6594	−0·21843	0·057322
0·07000	1·34448	0·02855	0·3317	0·6135	−0·21848	−0·07781
0·06000	1·41119	0·01412	0·4398	0·5649	−0·20369	−0·42141
0·05500	1·44054	0·00830	0·4949	0·5394	−0·18610	−0·7959
0·05000	1·46746	0·00362	0·5508	0·5130	−0·1549	−1·5593
0·04255	1·50134	0·00000	0·6353	0·4714	0·00000	

Table 6

NLR Quasi-Elliptical Profile

M_∞ = 0·7557
C_L = 0·254
t/c = 12·12%

Incidence α = 1·3217°

Leading Edge X_o = −1·48249
Y_o = 0·03733

ε_o = 0·625
α = 0·0275
T = 0·375
τ_1 = 0·1025
τ_c = 0·0622645
θ_c = −1·1855°
μ_2 = 0·4

Upper Surface

x	y	θ	dθ/ds	M	C_p
−1·48249	0·03733				
−1·48240	+0·03966	+1·51190	+16·12054	0·2247	+1·0248
−1·48172	+0·04578	+1·40921	+17·27832	0·3194	+0·9017
−1·48082	+0·05020	+1·32870	+18·38133	0·3932	+0·7817
−1·47981	+0·05377	+1·25866	+19·35241	0·4564	+0·6647
−1·47871	+0·05683	+1·19458	+20·07249	0·5130	+0·5508
−1·47753	+0·05957	+1·13416	+20·44617	0·5649	+0·4398
−1·47626	+0·06210	+1·07530	+20·47074	0·6135	+0·3317
−1·47328	+0·06691	+0·95938	+19·27070	0·7032	+0·1241
−1·47149	+0·06934	+0·90817	+17·77918	0·7454	+0·0245
−1·46892	+0·07245	+0·85536	+16·34220	0·7861	−0·0724
−1·46703	+0·07450	+0·80035	+14·58880	0·8257	−0·1666
−1·46420	+0·07726	+0·74584	+12·79539	0·8644	−0·2582
−1·45723	+0·08303	+0·64026	+9·84727	0·9393	−0·4336
−1·45268	+0·08624	+0·59105	+8·49794	0·9759	−0·5175
−1·44878	+0·08875	+0·55448	+7·59022	1·0000	−0·5721
−1·44698	+0·08984	+0·53936	+7·23004	1·0120	−0·5988
−1·44064	+0·09343	+0·49019	+6·18906	1·0476	−0·6780
−1·43333	+0·09711	+0·44365	+5·23477	1·0830	−0·7546
−1·42441	+0·10108	+0·39637	+4·41822	1·1180	−0·8290
−1·41352	+0·10534	+0·35003	+3·63585	1·1529	−0·9010
−1·41024	+0·10651	+0·33794	+3·40249	1·1616	−0·9187
−1·40616	+0·10791	+0·32362	+2·55575	1·1702	−0·9362
−1·39794	+0·11056	+0·29895	+2·61862	1·1847	−0·9651
−1·39618	+0·11109	+0·29430	+2·52249	1·1875	−0·9708
−1·39118	+0·11258	+0·28309	+2·28773	1·1933	−0·9822
−1·38668	+0·11386	+0·27138	+2·04510	1·1962	−0·9879
−1·35516	+0·12170	+0·22112	+1·19098	1·2019	−0·9993
−1·32694	+0·12759	+0·19201	+0·85600	1·1933	−0·9822
−1·30785	+0·13115	+0·17691	+0·72089	1·1875	−0·9708
−1·28386	+0·13523	+0·16121	+0·60739	1·1789	−0·9534
−1·26077	+0·13883	+0·14790	+0·53920	1·1702	−0·9362
−1·24002	+0·14179	+0·13608	+0·44021	1·1616	−0·9187
−1·20710	+0·14608	+0·12356	+0·38691	1·1529	−0·9010
−1·17760	+0·14958	+0·11271	+0·33805	1·1442	−0·8832
−1·14423	+0·15317	+0·10211	+0·29636	1·1355	−0·8653
−1·10251	+0·15720	+0·09070	+0·25716	1·1268	−0·8472
−1·05661	+0·16111	+0·07962	+0·22449	1·1180	−0·8290
−1·00535	+0·16492	+0·06878	+0·19725	1·1093	−0·8106
−0·94620	+0·16866	+0·05780	+0·17282	1·1005	−0·7921
−0·87185	+0·17250	+0·04576	+0·15210	1·0918	−0·7734
−0·79076	+0·17573	+0·03405	+0·13631	1·0830	−0·7546
−0·69275	+0·17844	+0·02141	+0·12369	1·0742	−0·7357
−0·58959	+0·18000	+0·00908	+0·11601	1·0653	−0·7166
−0·48320	+0·18032	−0·00302	+0·11213	1·0565	−0·6974
−0·37919	+0·17940	−0·01467	+0·11180	1·0476	−0·6780
−0·28166	+0·17744	−0·02554	+0·11381	1·0388	−0·6584
−0·19673	+0·17486	−0·03532	+0·11726	1·0299	−0·6388
−0·12099	+0·17184	−0·04432	+0·12136	1·0209	−0·6189
−0·05384	+0·16859	−0·05261	+0·12564	1·0120	−0·5989
+0·00588	+0·16522	−0·06021	+0·12950	1·0030	−0·5788
+0·02475	+0·16406	−0·06266	+0·13067	1·0000	−0·5721
+0·06109	+0·16169	−0·06748	+0·13294	0·9940	−0·5585
+0·11145	+0·15811	−0·07426	+0·13565	0·9850	−0·5381
+0·15857	+0·15446	−0·08073	+0·13775	0·9759	−0·5175
+0·20380	+0·15065	−0·08701	+0·13935	0·9668	−0·4967

Table 6 (continued)

Upper Surface (continued)

x	y	θ	dθ/ds	M	C_p
+0·24589	+0·14686	−0·09291	+0·14012	0·9577	−0·4758
+0·28539	+0·14307	−0·09844	+0·14017	0·9485	−0·4548
+0·32432	+0·13911	−0·10393	+0·13985	0·9393	−0·4336
+0·36349	+0·13492	−0·10947	+0·13939	0·9301	−0·4122
+0·39899	+0·13093	−0·11419	+0·13770	0·9208	−0·3907
+0·43502	+0·12671	−0·11913	+0·13592	0·9115	−0·3690
+0·47040	+0·12239	−0·12388	+0·13372	0·9022	−0·3471
+0·50438	+0·11808	−0·12839	+0·13096	0·8928	−0·3251
+0·53885	+0·11355	−0·13293	+0·12814	0·8834	−0·3030
+0·57244	+0·10899	−0·13720	+0·12469	0·8739	−0·2807
+0·60606	+0·10428	−0·14145	+0·12115	0·8644	−0·2582
+0·63915	+0·09949	−0·14548	+0·11713	0·8548	−0·2355
+0·67174	+0·09466	−0·14912	+0·11228	0·8452	−0·2127
+0·70428	+0·08971	−0·15273	+0·10729	0·8355	−0·1897
+0·73674	+0·08466	−0·15615	+0·10166	0·8257	−0·1666
+0·76897	+0·07953	−0·15945	+0·09577	0·8159	−0·1433
+0·80114	+0·07430	−0·16247	+0·08915	0·8061	−0·1198
+0·83303	+0·06903	−0·16516	+0·08165	0·7961	−0·0962
+0·86521	+0·06363	−0·16770	+0·07359	0·7861	−0·0724
+0·89659	+0·05828	−0·16992	+0·06572	0·7760	−0·0484
+0·92850	+0·05277	−0·17188	+0·05490	0·7659	−0·0243
+0·99110	+0·04181	−0·17466	+0·03181	0·7454	+0·0245
+1·02251	+0·03625	−0·17550	+0·01822	0·7350	+0·0491
+1·05406	+0·03065	−0·17580	−0·00049	0·7245	+0·0739
+1·08548	+0·02507	−0·17562	−0·01121	0·7139	+0·0989
+1·11687	+0·01951	−0·17489	−0·03436	0·7032	+0·1241
+1·17983	+0·00849	−0·17116	−0·08273	0·6815	+0·1749
+1·21161	+0·00304	−0·16801	−0·11380	0·6705	+0·2006
+1·24286	−0·00220	−0·16411	−0·15017	0·6594	+0·2265
+1·27473	−0·00739	−0·15869	−0·19519	0·6481	+0·2525
+1·30657	−0·01237	−0·15157	−0·25201	0·6367	+0·2787
+1·33848	−0·01710	−0·14230	−0·32529	0·6252	+0·3051
+1·37058	−0·02151	−0·13015	−0·42938	0·6135	+0·3317
+1·40291	−0·02549	−0·11361	−0·59427	0·6016	+0·3584
+1·43530	−0·02881	−0·08880	−0·93302	0·5896	+0·3584
+1·46928	−0·03083	−0·02069	−2·54159	0·5762	+0·4150

Lower Surface

x	y	θ	dθ/ds	M	C_p
−1·48249	+0·03733				
−1·48130	+0·02344	−1·38054	−14·81781	0·0000	+1·1510
−1·47532	+0·00580	−1·10835	−14·05751	0·2247	+1·0248
−1·47068	−0·00225	−0·98242	−12·67278	0·3194	+0·9017
−1·46556	−0·00908	−0·88180	−10·97414	0·3932	+0·7817
−1·45958	−0·01569	−0·79269	−9·04563	0·4564	+0·6647
−1·45233	−0·02246	−0·71227	−7·23349	0·5130	+0·5508
−1·44809	−0·02598	−0·67467	−6·42538	0·5394	+0·4949
−1·44336	−0·02963	−0·63878	−5·64966	0·5649	+0·4398
−1·43805	−0·03343	−0·60403	−4·96865	0·5896	+0·3854
−1·43209	−0·03739	−0·57062	−4·35483	0·6135	+0·3317
−1·42541	−0·04153	−0·53885	−3·81212	0·6367	+0·2787
−1·41786	−0·04588	−0·50777	−3·31208	0·6594	+0·2265
−1·40935	−0·05045	−0·47770	−2·89843	0·6815	+0·1749
−1·39971	−0·05525	−0·44856	−2·51604	0·7032	+0·1241
−1·38881	−0·06031	−0·42043	−2·18233	0·7245	+0·0739
−1·37189	−0·06749	−0·38379	−1·79911	0·7522	+0·0081
−1·36238	−0·07123	−0·36636	−1·63544	0·7659	−0·0243
−1·35458	−0·07417	−0·35317	−1·56326	0·7760	−0·0484
−1·34641	−0·07712	−0·34108	−1·41827	0·7861	−0·0724
−1·33440	−0·08127	−0·32390	−1·28454	0·7994	−0·1041
−1·32443	−0·08454	−0·31076	−1·18766	0·8093	−0·1277
−1·31053	−0·08888	−0·29440	−1·07918	0·8225	−0·1589
−1·29461	−0·09355	−0·27725	−0·97047	0·8355	−0·1897
−1·26315	−0·10200	−0·24819	−0·81627	0·8580	−0·2431
−1·24264	−0·10702	−0·23194	−0·73391	0·8707	−0·2732
−1·23645	−0·10847	−0·22747	−0·71256	0·8739	−0·2807
−1·21769	−0·11268	−0·21456	−0·65652	0·8834	−0·3030
−1·19056	−0·11834	−0·19735	−0·58420	0·8959	−0·3325
−1·17474	−0·12143	−0·18802	−0·54864	0·9022	−0·3471
−1·15729	−0·12466	−0·17855	−0·51283	0·9084	−0·3617
−1·13802	−0·12804	−0·16885	−0·47855	0·9146	−0·3762
−1·11573	−0·13172	−0·15846	−0·43798	0·9208	−0·3907

Table 6 (continued)

Lower Surface (continued)

x	y	θ	dθ/ds	M	C_p
-1·07514	-0·13785	-0·14141	-0·39266	0·9301	-0·4122
-1·05825	-0·14020	-0·13514	-0·36768	0·9332	-0·4198
-1·03910	-0·14273	-0·12824	-0·34720	0·9363	-0·4265
-1·01962	-0·14518	-0·12175	-0·32803	0·9393	-0·4336
-0·94786	-0·15316	-0·10039	-0·26868	0·9455	-0·4477
-0·87727	-0·15963	-0·08315	-0·22088	0·9485	-0·4548
-0·72179	-0·17009	-0·05240	-0·17372	0·9485	-0·4548
-0·60776	-0·17500	-0·03420	-0·14565	0·9455	-0·4477
-0·52913	-0·17726	-0·02331	-0·13348	0·9424	-0·4407
-0·46016	-0·17856	-0·01452	-0·12602	0·9393	-0·4336
-0·40048	-0·17921	-0·00723	-0·12132	0·9363	-0·4265
-0·34593	-0·17942	-0·00075	-0·11790	0·9332	-0·4193
-0·29441	-0·17931	+0·00524	-0·11540	0·9301	-0·4122
-0·20203	-0·17833	+0·01576	-0·11241	0·9239	-0·3979
-0·16069	-0·17759	+0·02036	-0·11137	0·9208	-0·3907
-0·08363	-0·17569	+0·02892	-0·11073	0·9146	-0·3762
-0·04975	-0·17464	+0·03273	-0·11030	0·9115	-0·3690
+0·07855	-0·16953	+0·04690	-0·11037	0·8991	-0·3398
+0·13466	-0·16672	+0·05310	-0·11051	0·8928	-0·3251
+0·18681	-0·16380	+0·05888	-0·11059	0·8865	-0·3104
+0·23576	-0·16078	+0·06430	-0·11071	0·8802	-0·2956
+0·28174	-0·15770	+0·06940	-0·11061	0·8739	-0·2807
+0·32585	-0·15453	+0·07428	-0·11044	0·8675	-0·2657
+0·36697	-0·15137	+0·07879	-0·10983	0·8612	-0·2506
+0·40711	-0·14812	+0·08323	-0·10922	0·8548	-0·2355
+0·44477	-0·14490	+0·08734	-0·10818	0·8484	-0·2203
+0·51663	-0·13832	+0·09505	-0·10542	0·8355	-0·1897
+0·55120	-0·13496	+0·09872	-0·10370	0·8290	-0·1743
+0·61656	-0·12827	+0·10538	-0·09924	0·8159	-0·1433
+0·64805	-0·12489	+0·10846	-0·09654	0·8093	-0·1277
+0·66350	-0·12319	+0·10995	-0·09501	0·8061	-0·1198
+0·72347	-0·11640	+0·11547	-0·08801	0·7928	-0·0883
+0·75261	-0·11299	+0·11798	-0·08390	0·7861	-0·0724
+0·78116	-0·10957	+0·12018	-0·07938	0·7794	-0·0564
+0·79516	-0·10787	+0·12121	-0·08204	0·7760	-0·0484
+0·85002	-0·10107	+0·12520	-0·06563	0·7625	-0·0162
+0·89066	-0·09588	+0·12808	-0·05716	0·7522	+0·0081
+0·91712	-0·09246	+0·12952	-0·04999	0·7454	+0·0245
+0·95611	-0·08734	+0·13125	-0·03801	0·7350	+0·0491
+0·99450	-0·08225	+0·13248	-0·02455	0·7245	+0·0739
+1·03237	-0·07719	+0·13319	-0·00906	0·7139	+0·0989
+1·06964	-0·07219	+0·13321	+0·00877	0·7032	+0·1241
+1·14280	-0·06244	+0·13111	+0·05337	0·6815	+0·1749
+1·17909	-0·05770	+0·12851	+0·08210	0·6705	+0·2006
+1·21511	-0·05311	+0·12489	+0·11651	0·6594	+0·2265
+1·25111	-0·04867	+0·11992	+0·15923	0·6481	+0·2525
+1·28649	-0·04452	+0·11360	+0·21161	0·6367	+0·2787
+1·32197	-0·04062	+0·10484	+0·27999	0·6252	+0·3051
+1·35735	-0·03710	+0·09323	+0·37728	0·6135	+0·3317
+1·39261	-0·03407	+0·07728	+0·52496	0·6016	+0·3584
+1·42819	-0·03171	+0·05341	+0·82129	0·5896	+0·3854
+1·46928	-0·03083	-0·02069	+2·29761	0·5762	+0·4150

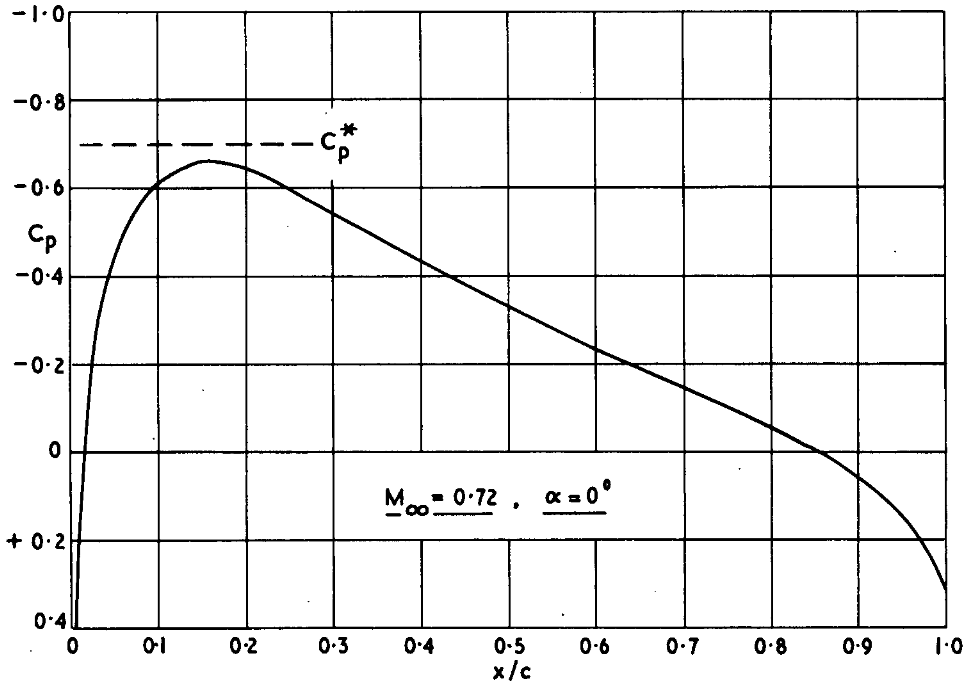

FIG.1 Aerofoil NACA 0012

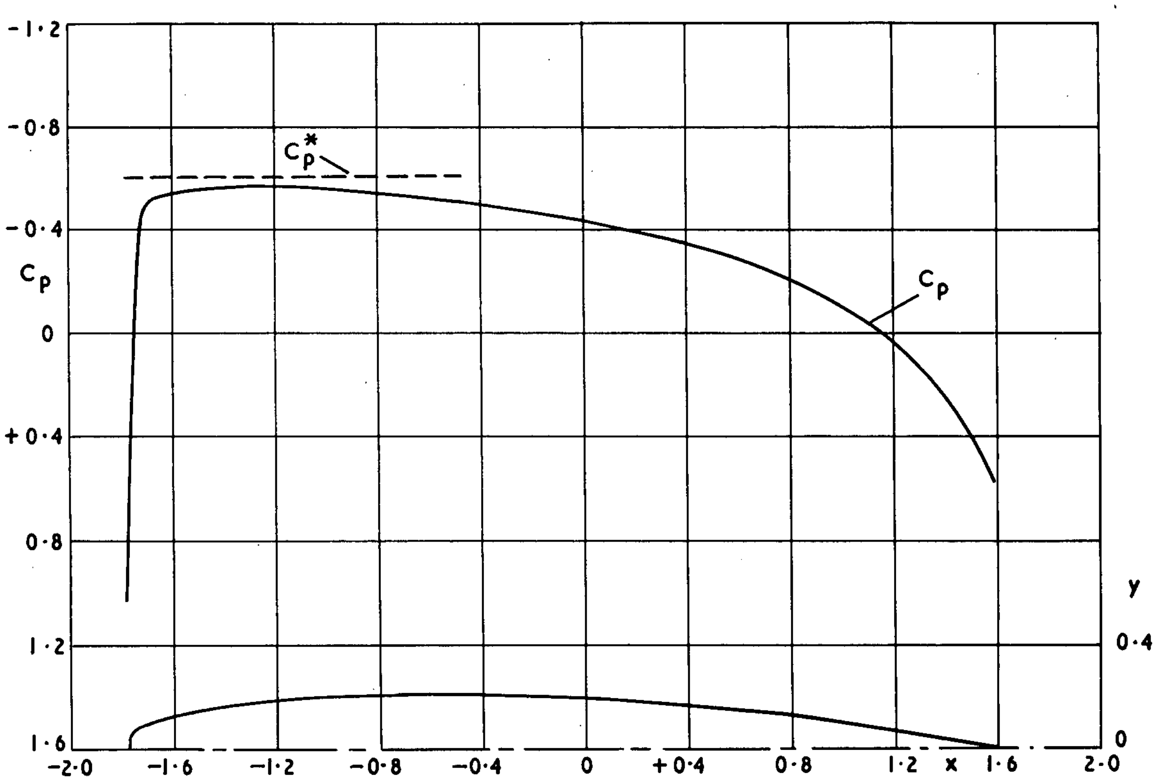

FIG.2 NLR Section 0·10–0·75–1·25 : $M_\infty = 0·745$, $\alpha = 0$

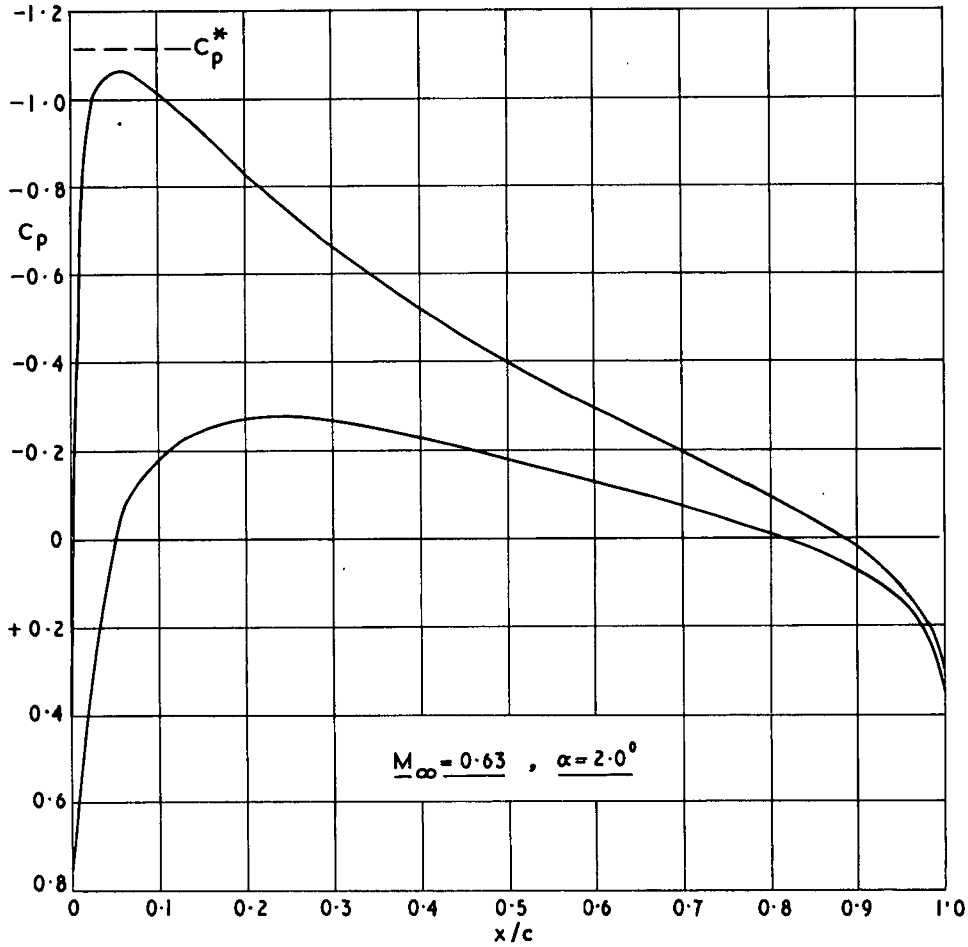

FIG. 3 Aerofoil NACA 0012

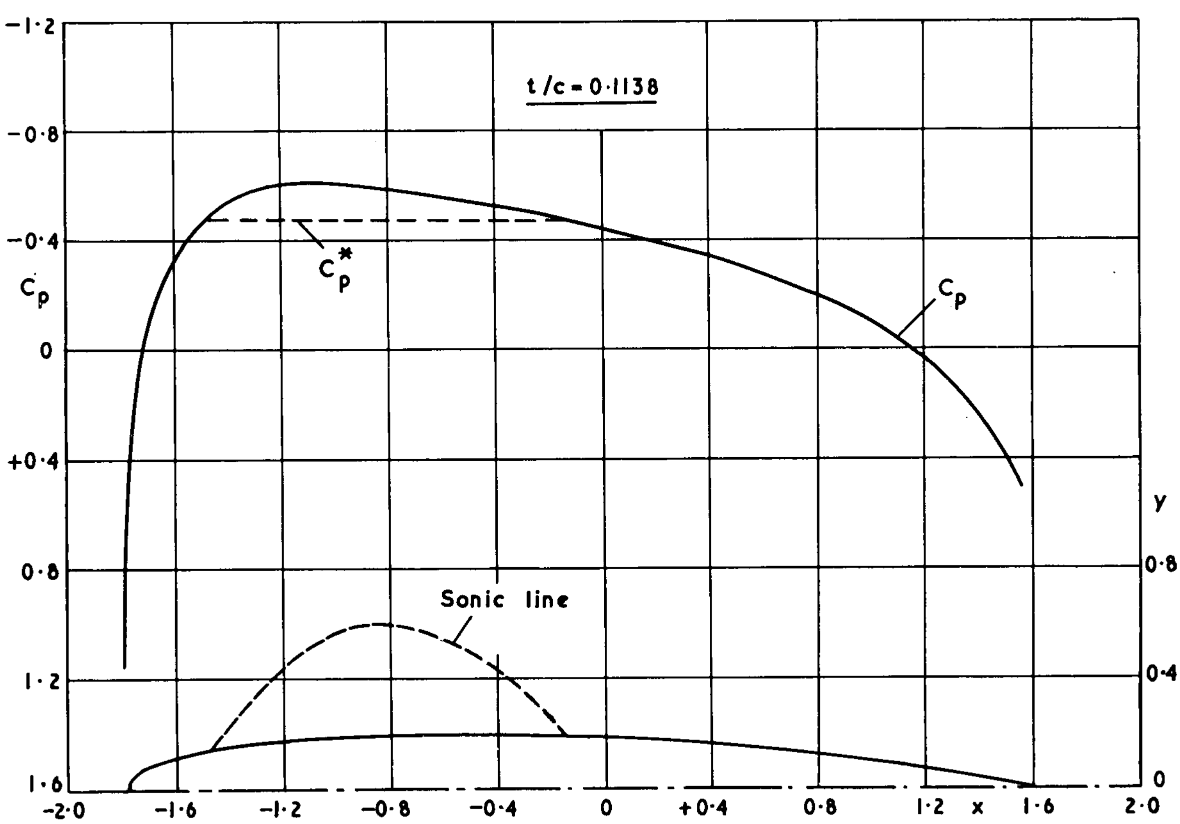

FIG. 4 NLR Section 0·1100–0·75–0·9: $M_\infty = 0·786$, $\alpha = 0$

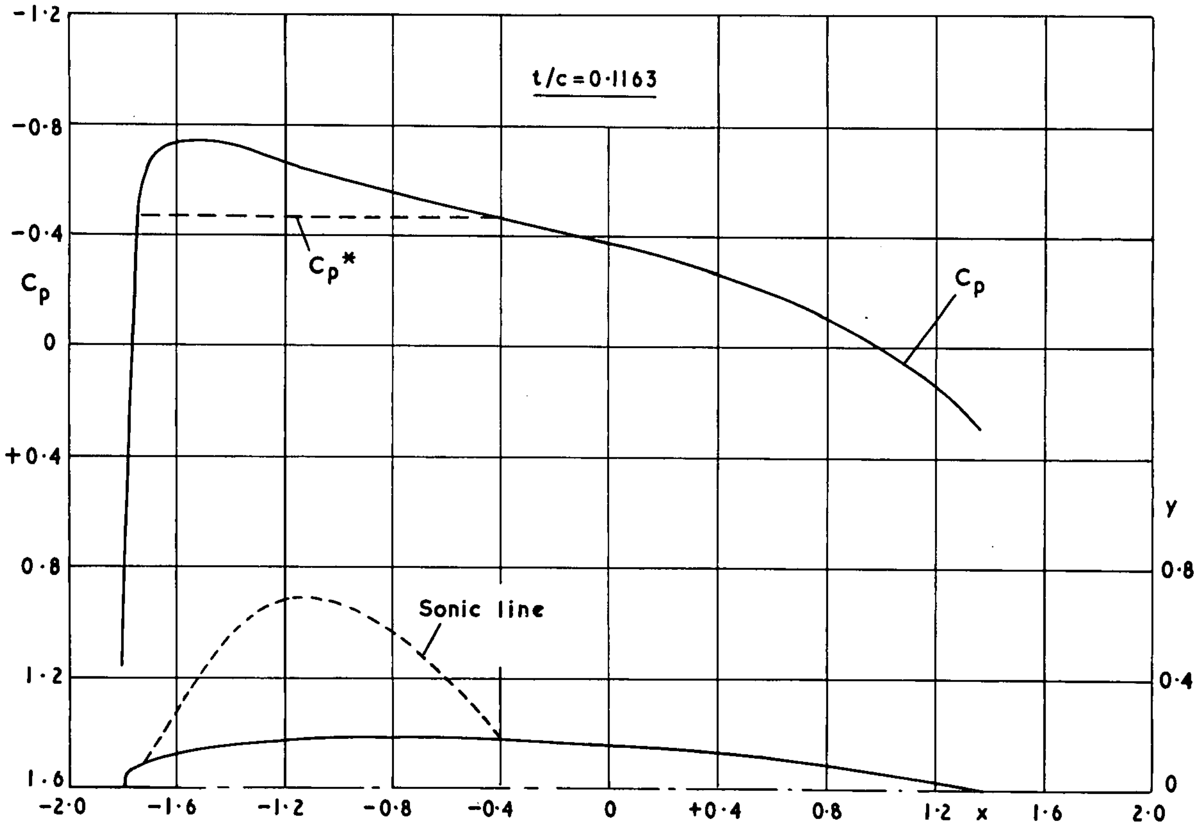

FIG. 5 NLR Section 0·11−0·75−1·25 : $M_\infty = 0·786$, $\alpha = 0$

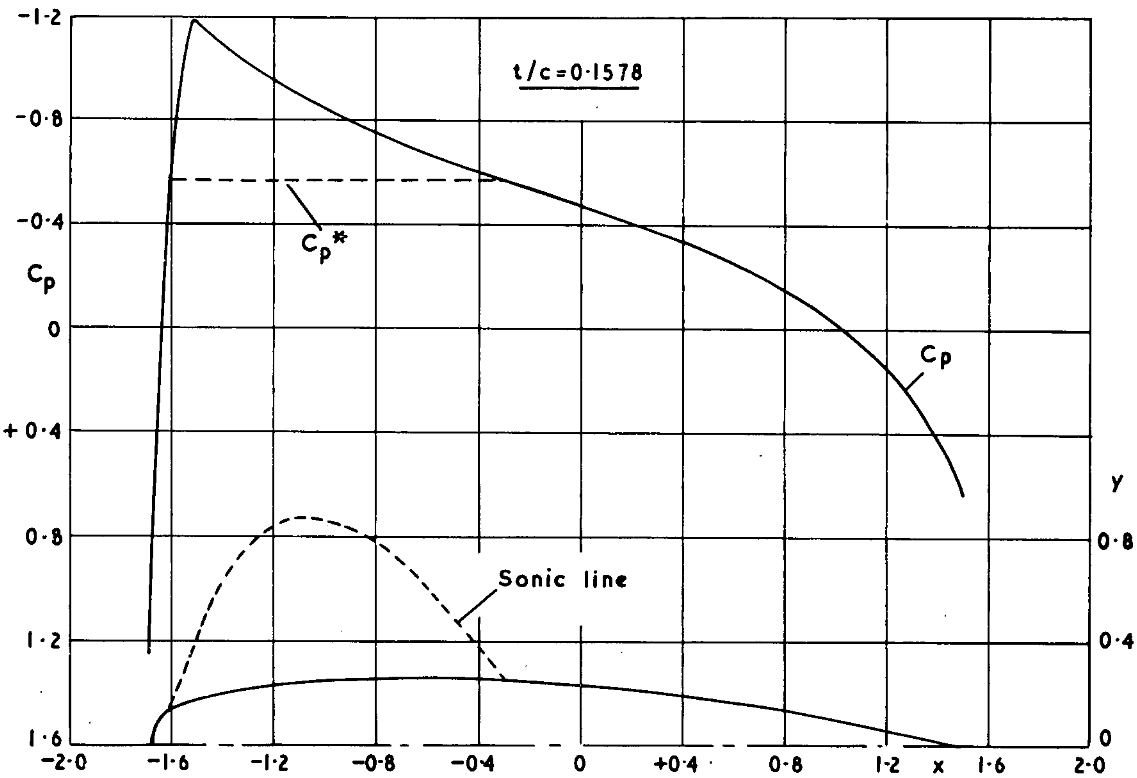

FIG 6 NLR Section 0·1025−0·675−1·375 : $M_\infty = 0·756$, $\alpha = 0$

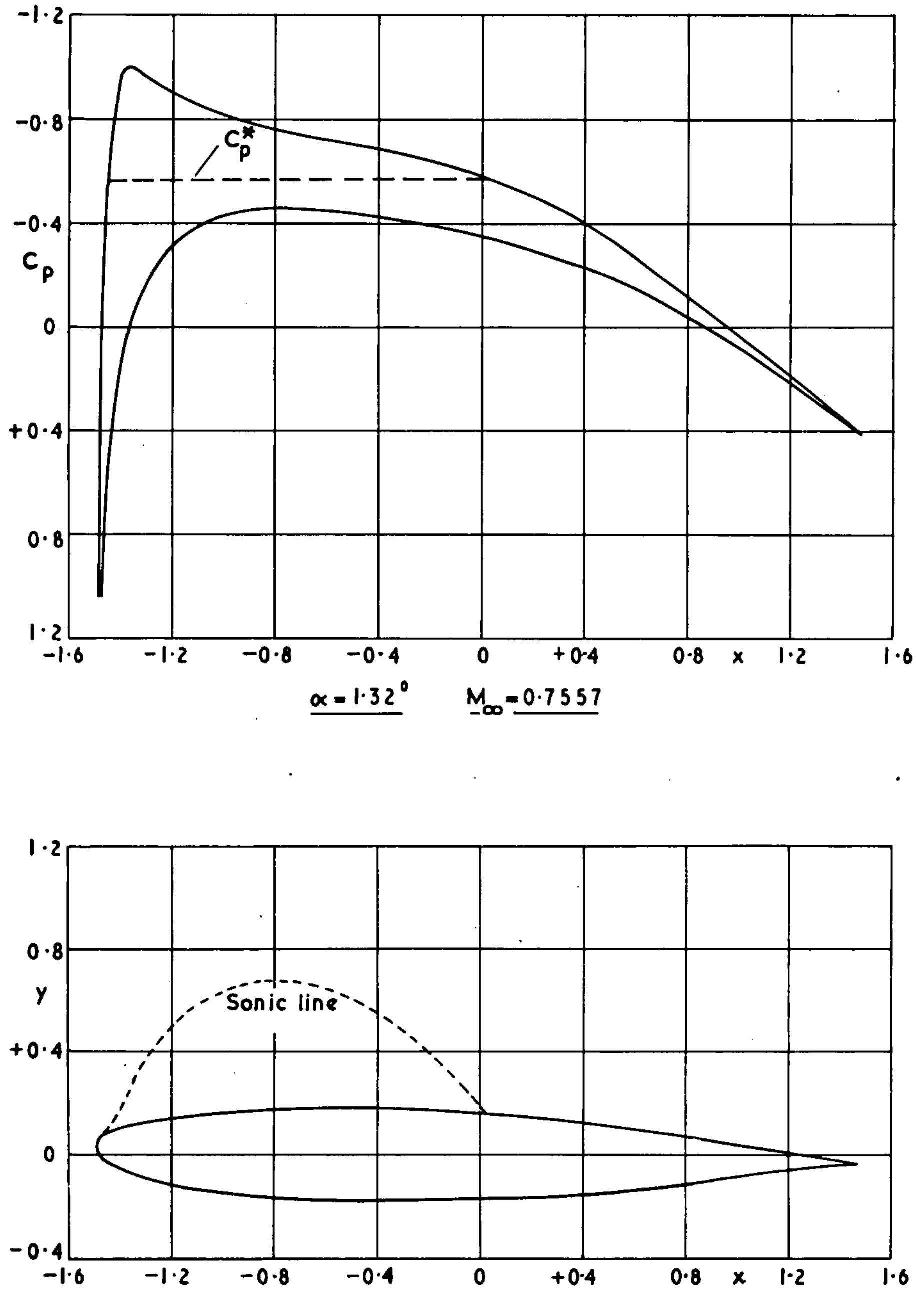

FIG.7 NLR lifting aerofoil (t/c = 0·1212)

AGARD Report No. 575
North Atlantic Treaty Organization, Advisory Group for Aerospace Research and Development
TEST CASES FOR NUMERICAL METHODS IN TWO-DIMENSIONAL TRANSONIC FLOWS
R. C. Lock
Published November 1970
22 pages incl. figs.

In order to provide test cases for the development of numerical methods for the computation of two-dimensional transonic flows round aerofoils, 6 aerofoil shapes have been selected for which accurate solutions are available. These include both symmetrical and cambered profiles, non-lifting and lifting, in subcritical and supercritical (shock-free) flow.

This Report was prepared at the request of the Fluid Dynamics Panel of AGARD.

533.69.01:533.6.011.35

AGARD Report No. 575
North Atlantic Treaty Organization, Advisory Group for Aerospace Research and Development
TEST CASES FOR NUMERICAL METHODS IN TWO-DIMENSIONAL TRANSONIC FLOWS
R. C. Lock
Published November 1970
22 pages incl. figs

In order to provide test cases for the development of numerical methods for the computation of two-dimensional transonic flows round aerofoils, 6 aerofoil shapes have been selected for which accurate solutions are available. These include both symmetrical and cambered profiles, non-lifting and lifting, in subcritical and supercritical (shock-free) flow.

This Report was prepared at the request of the Fluid Dynamics Panel of AGARD.

533.69.01:533.6.011.35

AGARD Report No. 575
North Atlantic Treaty Organization, Advisory Group for Aerospace Research and Development
TEST CASES FOR NUMERICAL METHODS IN TWO-DIMENSIONAL TRANSONIC FLOWS
R. C. Lock
Published November 1970
22 pages incl. figs.

In order to provide test cases for the development of numerical methods for the computation of two-dimensional transonic flows round aerofoils, 6 aerofoil shapes have been selected for which accurate solutions are available. These include both symmetrical and cambered profiles, non-lifting and lifting, in subcritical and supercritical (shock-free) flow.

This Report was prepared at the request of the Fluid Dynamics Panel of AGARD.

533.69.01:533.6.011.35

AGARD Report No. 575
North Atlantic Treaty Organization, Advisory Group for Aerospace Research and Development
TEST CASES FOR NUMERICAL METHODS IN TWO-DIMENSIONAL TRANSONIC FLOWS
R. C. Lock
Published November 1970
22 pages incl. figs.

In order to provide test cases for the development of numerical methods for the computation of two-dimensional transonic flows round aerofoils, 6 aerofoil shapes have been selected for which accurate solutions are available. These include both symmetrical and cambered profiles, non-lifting and lifting, in subcritical and supercritical (shock-free) flow.

This Report was prepared at the request of the Fluid Dynamics Panel of AGARD.

533.69.01:533.6.011.35

AGARD Report No.575
North Atlantic Treaty Organization, Advisory Group for Aerospace Research and Development
TEST CASES FOR NUMERICAL METHODS IN TWO-DIMENSIONAL TRANSONIC FLOWS
R.C.Lock
Published November 1970
22 pages incl. figs.

In order to provide test cases for the development of numerical methods for the computation of two-dimensional transonic flows round aerofoils, 6 aerofoil shapes have been selected for which accurate solutions are available. These include both symmetrical and cambered profiles, non-lifting and lifting, in subcritical and supercritical (shock-free) flow.

This Report was prepared at the request of the Fluid Dynamics Panel of AGARD.

533.69.01:533.6.011.35

AGARD Report No.575
North Atlantic Treaty Organization, Advisory Group for Aerospace Research and Development
TEST CASES FOR NUMERICAL METHODS IN TWO-DIMENSIONAL TRANSONIC FLOWS
R.C.Lock
Published November 1970
22 pages incl. figs

In order to provide test cases for the development of numerical methods for the computation of two-dimensional transonic flows round aerofoils, 6 aerofoil shapes have been selected for which accurate solutions are available. These include both symmetrical and cambered profiles, non-lifting and lifting, in subcritical and supercritical (shock-free) flow.

This Report was prepared at the request of the Fluid Dynamics Panel of AGARD.

533.69.01:533.6.011.35

AGARD Report No.575
North Atlantic Treaty Organization, Advisory Group for Aerospace Research and Development
TEST CASES FOR NUMERICAL METHODS IN TWO-DIMENSIONAL TRANSONIC FLOWS
R.C.Lock
Published November 1970
22 pages incl. figs.

In order to provide test cases for the development of numerical methods for the computation of two-dimensional transonic flows round aerofoils, 6 aerofoil shapes have been selected for which accurate solutions are available. These include both symmetrical and cambered profiles, non-lifting and lifting, in subcritical and supercritical (shock-free) flow.

This Report was prepared at the request of the Fluid Dynamics Panel of AGARD.

533.69.01:533.6.011.35

AGARD Report No.575
North Atlantic Treaty Organization, Advisory Group for Aerospace Research and Development
TEST CASES FOR NUMERICAL METHODS IN TWO-DIMENSIONAL TRANSONIC FLOWS
R.C.Lock
Published November 1970
22 pages incl. figs.

In order to provide test cases for the development of numerical methods for the computation of two-dimensional transonic flows round aerofoils, 6 aerofoil shapes have been selected for which accurate solutions are available. These include both symmetrical and cambered profiles, non-lifting and lifting, in subcritical and supercritical (shock-free) flow.

This Report was prepared at the request of the Fluid Dynamics Panel of AGARD.

533.69.01:533.6.011.35

NATIONAL DISTRIBUTION CENTRES FOR UNCLASSIFIED AGARD PUBLICATIONS

Unclassified AGARD publications are distributed to NATO Member Nations through the unclassified National Distribution Centres listed below

BELGIUM
General J. DELHAYE
Coordinateur AGARD – V.S.L.
Etat Major Forces Aériennes
Caserne Prince Baudouin
Place Dailly, Bruxelles 3

CANADA
Director of Scientific Information Services
Defence Research Board
Department of National Defence – 'A' Building
Ottawa, Ontario

DENMARK
Danish Defence Research Board
Østerbrogades Kaserne
Copenhagen Ø

FRANCE
O.N.E.R.A. (Direction)
29, Avenue de la Division Leclerc
92, Châtillon-sous-Bagneux

GERMANY
Zentralstelle fur Lüftfahrtdokumentation und Information
Maria-Theresia Str. 21
8 München 27
Attn: Dr Ing. H.J. RAUTENBERG

GREECE
Hellenic Armed Forces Command
D Branch, Athens

ICELAND
Director of Aviation
c/o Flugrad
Reykjavik

ITALY
Aeronautica Militare
Ufficio del Delegato Nazionale all' AGARD
3, Piazzale Adenauer
Roma/EUR

LUXEMBOURG
Obtainable through BELGIUM

NETHERLANDS
Netherlands Delegation to AGARD
National Aerospace Laboratory, NLR
Attn: Mr A.H. GEUDEKER
P.O. Box 126
Delft

NORWAY
Norwegian Defense Research Establishment
Main Library, c/o Mr P.L. EKERN
P.O. Box 25
N-2007 Kjeller

PORTUGAL
Direccao do Servico de Material
da Forca Aerea
Rua de Escola Politecnica 42
Lisboa
Attn: Brig. General Jose de Sousa OLIVEIRA

TURKEY
Turkish General Staff (ARGE)
Ankara

UNITED KINGDOM
Ministry of Technology Reports Centre
Station Square House
St. Mary Cray
Orpington, Kent BR5 3RE

UNITED STATES
National Aeronautics and Space Administration (NASA)
Langley Field, Virginia 23365
Attn: Report Distribution and Storage Unit

* * *

If copies of the original publication are not available at these centres, the following may be purchased from:

Microfiche or Photocopy
National Technical
Information Service (NTIS)
5285 Port Royal Road
Springfield
Virginia 22151, USA

Microfiche
ESRO/ELDO Space
Documentation Service
European Space
Research Organization
114, Avenue de Neuilly
92, Neuilly-sur-Seine, France

Microfiche
Ministry of Technology
Reports Centre
Station Square House
St. Mary Cray
Orpington, Kent BR5 3RE
England

The request for microfiche or photocopy of an AGARD document should include the AGARD serial number, title, author or editor, and publication date. Requests to CFSTI should include the NASA accession report number.

Full bibliographical references and abstracts of the newly issued AGARD publications are given in the following bi-monthly abstract journals with indexes:

Scientific and Technical Aerospace Reports (STAR)
published by NASA,
Scientific and Technical Information Facility,
P.O. Box 33, College Park,
Maryland 20740, USA

United States Government Research and Development
Report Index (USGDRI), published by the Clearinghouse
for Federal Scientific and Technical Information,
Springfield, Virginia 22151, USA

Printed by Technical Editing and Reproduction Ltd
Harford House, 7-9 Charlotte St, London. W1P 1HD